Broadband superluminescent diodes based on multiple InGaAs/GaAs quantum well-dot layers

© M.V. Maximov[1], Yu.M. Shernyakov[2], G.O. Kornyshov[1], O.I. Simchuk[1], N.Yu. Gordeev[2], A.A. Beckman[2], A.S. Payusov[2], S.A. Mintairov[2], N.A. Kalyuzhnyy[2], M.M. Kulagina[2], A.E Zhukov[3]

[1] Alferov University,
194021 St. Petersburg, Russia
[2] Ioffe Institute,
194021 St. Petersburg, Russia
[3] HSE University,
190008 St. Petersburg, Russia
E-mail: maximov.mikh@gmail.com

Received May 26, 2023
Revised June 16, 2023
Accepted June 23, 2023

We have studied superluminescent diodes with simplified design and active region based on 5 or 7 layers of InGaAs/GaAs quantum well-dots (QWDs). Emission peaks of the individual QWD layers are shifted with respect to each other by 15−35 nm to provide as wide as possible emission line in a superluminescent mode with central wavelength of about 1 μm without significant spectral dips. For superluminescent diodes with the active region based on 5 and 7 QWD layers, the maximal value of full width at half maximum of emission spectrum was 92 and 103 nm respectively.

Keywords: quantum well dots, broadband radiation source, superluminescent diode.

DOI: 10.61011/SC.2023.04.56429.5262

1. Introduction

Superluminescent diodes (SLDs) are of considerable interest for investigating the fundamentals of light emission and amplification in matter, and are key components for a large number of modern optical systems. The active area of such a device should provide high luminescence intensity, while the optical feedback in the resonator is suppressed, and the laser generation mode is not achieved.

One of the important practical applications of SLD is optical coherent tomography (OCT) systems in the time domain, based on the use of a broadband light source and a mechanically moving reference mirror. The key element of OCT is the SLD, the basic most general requirements for which are as follows: 1) large width of the emission spectrum; 2) intensity modulations (maxima and dips) in the spectrum should be minimized; 3) high output power. The wider the bandwidth of the light source, the better the resolution and contrast of biological tissues in the OCT image. Spectral dips and maxima in the emission spectrum are undesirable for OCT systems as well as other applications, as they can be a source of false images. The third requirement, i. e. high output power, arises from the need to increase the dynamic range and achieve the highest possible sensitivity when visualizing weakly scattering areas deep within the samples.

Broadband optical sources from 950 to 1150 nm are essential for realizing OCT systems capable of scanning the retina and other organs composed predominantly of water. The water absorption spectrum has a local minimum in the area of 1.06 μm [1], so the use of such sources reduces the effect of moisture on the results of biological objects. Since water-containing substances have zero dispersion around 1 μm, examination of objects at these wavelengths reduces the effect of dispersion on the resolving power of the OCT [2] system. It should also be noted that for the same half-width of the emission line, a shorter-wavelength SLD will provide better spatial depth resolution, which is proportional to the ratio of the square of the emission wavelength to the width of the spectrum [3].

Besides OCT, superluminescent diodes are widely used in other fields of science and technology. An important application for 1−1.1 μm optical-band SLDs is fiber gyroscopes for unmanned ground transport systems. The technical requirements for such systems are less stringent than for unmanned aerial vehicles, but ground-based systems must be sufficiently cheap, reliable, and operate in the IR spectral range that is relatively safe for vision. The use of silicon photodetectors and charge-coupled device (CCD) arrays, whose sensitivity drops rapidly as the wavelength increases beyond 1100 nm (which defines the required spectral range of SLD emission), has a significant effect on reducing the price of such systems. In addition, SLDs are promising for optical data transmission, random number generation, and as light sources for imaging applications ranging from next-generation microscopes and laser projectors to digital holography and photolithography. SLDs have a wide range of applications for scientific research, particularly in spectroscopy.

Traditionally, InGaAs/GaAs quantum wells (QWs) are used as the active area of radiation sources in the spectral area from 950 to 1100 nm. However, the development

of wideband SLDs based on QWs is quite a challenging task. The spectral width of QW radiation is relatively small (10−15 nm), and the growth of the multilayer active area requires the use of complex technology for elastic stress compensation. Another problem is related to the decrease in the density of carriers in the QW with their distance from the *p*-emitter [4]. This leads to the fact that the gain and electroluminescence spectra are dominated by the contribution from the QW closest to the *p*-emitter. It should be noted that this effect is less pronounced in quantum dots. A bipolar cascade superluminescent diode whose active area consisted of four strained InGaAs/GaAs QWs with ground state emission wavelengths of 1050, 1100, 1000, and 950 nm (listed according to the location from *n*-emitter to *p*-emitter) was investigated in paper [5]. The SLD contained a tunneling $p-n$ transition in the center of the active area, serving to minimize the non-uniform distribution of carriers between the different QWs. The full-width at half maximum (FWHM) of this SLD in continuous mode reaches 180 nm, with an output power of only 0.65 mW. With pulse pumping, an output power of 19 mW was achieved at a spectral half-width of 14 nm.

Recently, self-organized InGaAs/GaAs quantum dots (QDs) have been used as the active area of broadband SLDs. The inhomogeneous broadening of the QD ensemble, associated with their dispersion in shape and size, causes a rather large half-width of the emission line, which is typically ~ 60 nm. An even greater increase in the width of the SLD emission spectrum and a smooth intensity profile without significant modulations can be realized by using the so-called chirped multilayer active area, in which the maxima in the emission spectra of individual QD layers are shifted in such a way as to fill the gaps between the lines of the ground and excited states of each QD layer [6,7]. So-called dot-in-well (DWELL) dots are often used as the active area of infrared SLDs, obtained by overlaying the initial InAs-quantum dots with an InGaAs layer, the composition and thickness of which can vary [8]. The largest emission spectrum widths were achieved for the optical range 1.2 μm. Thus, in [9], an SLD with a hybrid active area consisting of one QW $In_{0.34}Ga_{0.66}As$ and six InAs/InGaAs/GaAs QD (DWELL) layers was proposed with a full width of half maximum of 290 nm. The output power was 2.4 mW.

For the optical range of 1.1 μm, a half-width spectrum of 140 nm is obtained at an emission power of 3 mW [10] at the output of a single-mode fiber. 4 chirped QD layers of different heights, repeated 2 times, were used as the active area. The SLD design was a 1 mm long inclined stripe with a waveguide extending laterally.

It should be noted that the use of In(Ga)As/GaAs QDs as the active area of $\sim 1.1\,\mu$m infrared SLDs is associated with certain difficulties. In such QDs, the localization of charge carriers relative to the InGaAs wetting layer is rather small, so with increasing pump current, the peak from the wetting layer (~ 960 nm) quickly begins to dominate in the spectrum against the background of saturating long-wavelength peaks of the QD states. As a consequence, at high currents corresponding to high output power, the spectra are severely narrowed. It is therefore difficult to achieve high power and a broad spectrum of radiation at the same time. In paper [11], an SLD of the optical range 980−1060 nm with maximum half-width of emission spectra ~ 80 nm is demonstrated.

The method of intermixing atoms during thermal annealing (intermixing) can be used to reduce the band gap width of QDs and the corresponding shift of the central wavelength of radiation to the short-wavelength area. The SLD based on multilayer QD structure obtained by rapid thermal annealing showed an electroluminescence bandwidth of 146 nm at 3 dB with a central wavelength of 984 nm and a continuous output power of 15 mW [12].

An interesting way to increase the half-width of the SLD emission spectrum is to increase the operating temperature, which increases the carrier population of excited QD states. In paper [13], SLDs operating at 180°C with an emission spectrum half-width of 270 nm and an output power of 0.34 mW are demonstrated. However, the degradation characteristics of devices operating at such a high temperature require a separate study.

In this paper, nanostructures of fractional (0D/2D) dimensionality — quantum well-dots (QWDs) [14] were used as the active area of SLDs for the first time. They have a record high material gain ($1.1 \cdot 10^4\,cm^{-1}$) [15] and a broader emission spectrum compared to QWs. The possibility of dislocation-free growth of 10−15 layers of QWDs in the active area contributes to the realization of broad and flat (without strong intensity modulations) emission spectra in chirped structures and high output power. In QWDs, unlike QDs, ground state saturation is not observed up to very high injection currents. Thus, the emission spectrum of multilayer chirped SLDs on QWDs will not change significantly with pump current due to the increased contribution of excited states. It is expected that in QWDs, due to their similarity to QDs, the problem of carrier density decrease in individual layers in the active area with their distance from the *p*-emitter will be less pronounced than in QW.

2. Samples and experiment procedure

The heterostructures were synthesized by metal-organic vapour phase epitaxy (MOVPE) on n^+-GaAs substrates and represented the following sequence of layers: the lower *n*-cladding $Al_{0.25}Ga_{0.75}As:Si$ ($2 \cdot 10^{18}\,cm^{-3}$) with a thickness of 1450 nm, a GaAs waveguide with a total thickness of 440 nm, in the middle of which there was the active area with QWD, the upper *p*-doped cladding $Al_{0.25}Ga_{0.75}As:Zn$ ($2 \cdot 10^{18}\,cm^{-3}$) with a thickness of 1060 nm and the contact layer GaAs with a thickness of 150 nm. The waveguide thickness was smaller than the cutoff of the 2nd order vertical optical mode. Near the waveguide layer,

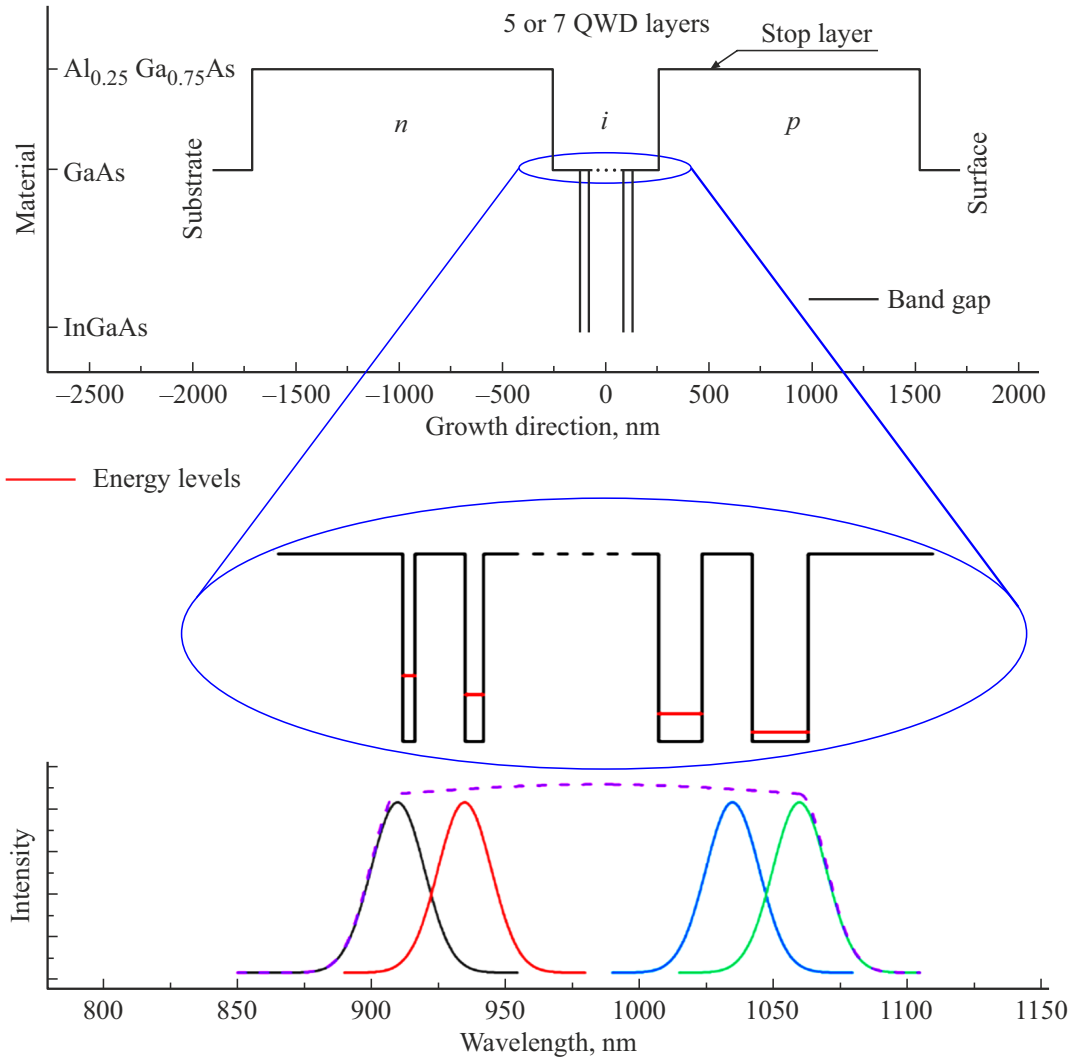

Figure 1. Schematic representation of the gap structure and emission spectrum of the epitaxial structure of superluminescent diodes with chirped layers QWs.

the doping level was reduced to $5 \cdot 10^{17}$ cm^{-3} to reduce optical losses. To enable precision etching, an InGaP stop layer was inserted into the top $Al_{0.25}Ga_{0.75}As$ cladding at a distance of 260 nm from the waveguide, which can be used to fabricate spatially single-mode waveguides. The active area was either 5 (5QWD structure) or 7 (7QWD structure) layers of QWDs. QWDs were formed by deposition of 2 to 8 monolayers (monolayers, MLs) of $In_{0.4}Ga_{0.6}As$ on substrates GaAs (100), misoriented by 6° along the direction to (111). The use of misoriented substrates, optimal temperature and growth rate promoted the formation of a high-density array of In-enriched areas inside the In-depleted InGaAs layer, t. e. QWD. The technology and optical properties of QWDs are described in detail in our paper [14]. The photoluminescence (PL) maxima of the layers were shifted relative to each other. In the 5QWD structure, the nominal amounts of deposited $In_{0.4}Ga_{0.6}As$ (wavelengths of emission maxima) of the individual QWD layers were 4 (985 nm), 5 (1015 nm), 6 (1015 nm), 6 (1040 nm), 7 (1060 nm), and 8ML (1075 nm), in structure 7QWD 2 (925 nm), 3 (950 nm), 4 (985 nm), 5 (1015 nm), 6 (1040 nm), 7 (1060 nm), and 8ML (1075 nm). The layers are listed according to their location from *n*- to *p*-cladding (Fig. 1). The wavelengths of emission maxima of individual QWD layers were estimated from measurements of photoluminescence spectra of heterostructures with single QWD layers grown during preliminary calibrations. The distance between the individual QWD layers in the GaAs waveguide was 40 nm. It should be noted that in multilayer structures, elastic stress fields can change the gap structure of QWDs and lead to a change in the spectral position of the maxima of the PL line compared to a structure containing only one similar layer QWD [16].

SLDs were fabricated in an tilted geometry with the stripe making an angle 10.5° to the normal to the output face of the SLD (Fig. 2, *a*). The width of the SLD stripe was

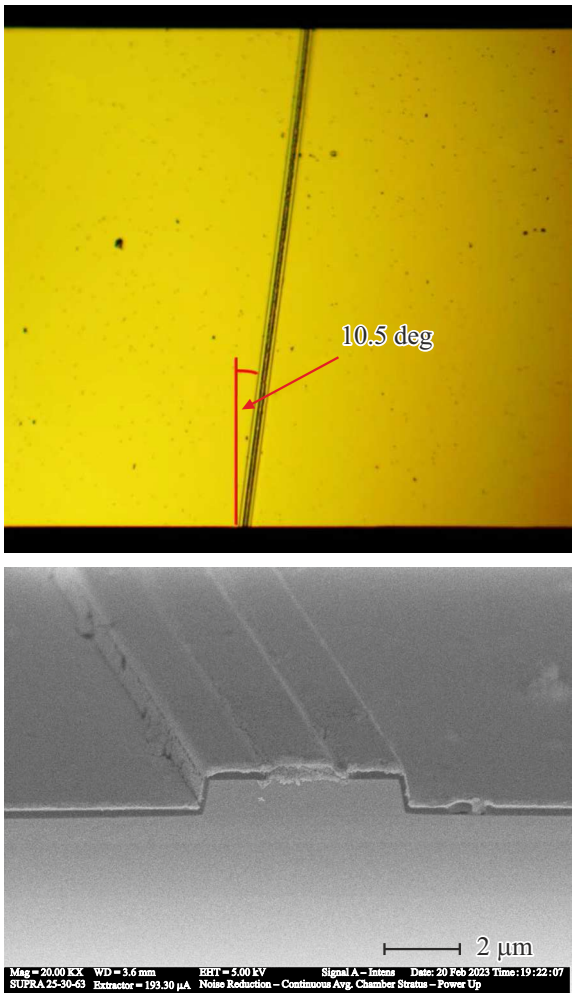

Figure 2. Images of the upper (a) and side (b) surface of the SLD obtained by optical and scanning-electron microscope, respectively.

5 μm, and the etch depth limited by the presence of the stop layer was 950 nm (Fig. 2, b). No antireflection coatings were applied to the facets. The lengths of the individual chips obtained by cleaving the wafer with contacts were 0.25 and 0.3 mm. The short length and tilted geometry of SLDs allow to significantly increase the threshold of unwanted laser generation while maintaining the amplified spontaneous emission mode up to high injection currents. The measurements were carried out in pulse mode (pulse duration 0.3 μs, repetition rate 2 kHz) at room temperature. An MDR-2 monochromator and an InGaAs G12180-250A InGaAs PIN photodiode were used to record the SLD spectra. It should be noted that the length of the devices investigated in this paper is much shorter than that of typical SLDs. This is because the objective of this paper was to investigate and optimize the active area in terms of the emission spectrum width, and an increase in power can be achieved by using standard long length SLD designs, antireflection mirrors, and an additional optical amplifier [17–19] section.

3. Results and discussion

Fig. 3 shows the electroluminescence spectra of SLD 5QWD and SLD 7QWD as a function of pump current. The nominal positions of the maxima of individual QWD layers are marked by vertical lines. At low pump currents, only the long-wavelength peak (1070–1075 nm) from the layer of the QWD with the highest carrier localization energy is present in the spectrum. As the injection current increases, the contribution of shorter-wavelength peaks from QWD layers with lower carrier localization energy gradually increases, and the total width of the electroluminescence (EL) spectrum increases (Fig. 4, a). The slowing down of the half-width growth with current is associated with the onset of stimulated emission in the spectral range corresponding to the PL maxima of QWD layers 985, 1015, 1040, 1060, and 1075 nm. When the current is further increased, relatively narrow peaks of stimulated emission appear in the EL spectra of both SLDs. For the 5QWD SLD, the maximum of the stimulated emission peak is at a wavelength of 1055 nm; in the case of the 7QWD SLD, it is shifted by 10 nm to the short-wavelength area (1045 nm). An increase in the intensity of the stimulated emission peaks leads to a decrease in the half-width of the EL spectra (Fig. 4, a). For the 5QWD SLD, the maximum half-width of the spectrum is 92 nm and is achieved at an injection current of 150 mA. Increasing the number of QWD layers in the active area from 5 to 7 allows increasing the half-width of the emission spectrum up to 103 nm in the 7QWD SLD, while the maximum FWHM value is achieved at a higher current (200 mA) than in the case of 5QWD SLD.

In an SLD with an active area based on 5 layers of QWDs, all layers contribute to the maximum half-width at half height. However, the spectrum does not have a flat top, which is desirable for broadband SLDs. The spectral width at the 90% intensity level is 41 nm. This is due to the fact that the main contribution to the spectrum width at the 90% intensity level is made only by the QWD layers emitting at wavelengths of 1040 and 1060 nm, while the contribution of other layers is much smaller. In an SLD with an active area based on 7 layers of QWDs, the main contribution to the maximum spectral width at the 90% level comes from four layers of QWDs emitting at wavelengths of 985, 1015, 1040, and 1060 nm, which leads to higher values of this value, which is 62 nm. The contribution of QWD layers emitting at wavelengths of 925 and 950 nm to the short-wavelength part of the total emission spectrum is very small. This fact may be due to two reasons. The former is analogous to the previously mentioned decrease in the density of carriers in the QW with their distance from the p-cladding [4]. This causes the gain and EL spectra to be dominated by the contribution from the QWDs closest to the p-cladding. The second reason may be related to the fact that thermal ejection of electrons and holes from QWDs with lower carrier localization energy and their recapture in QWDs with higher localization energy leads to lower EL lower EL intensity of the former ones.

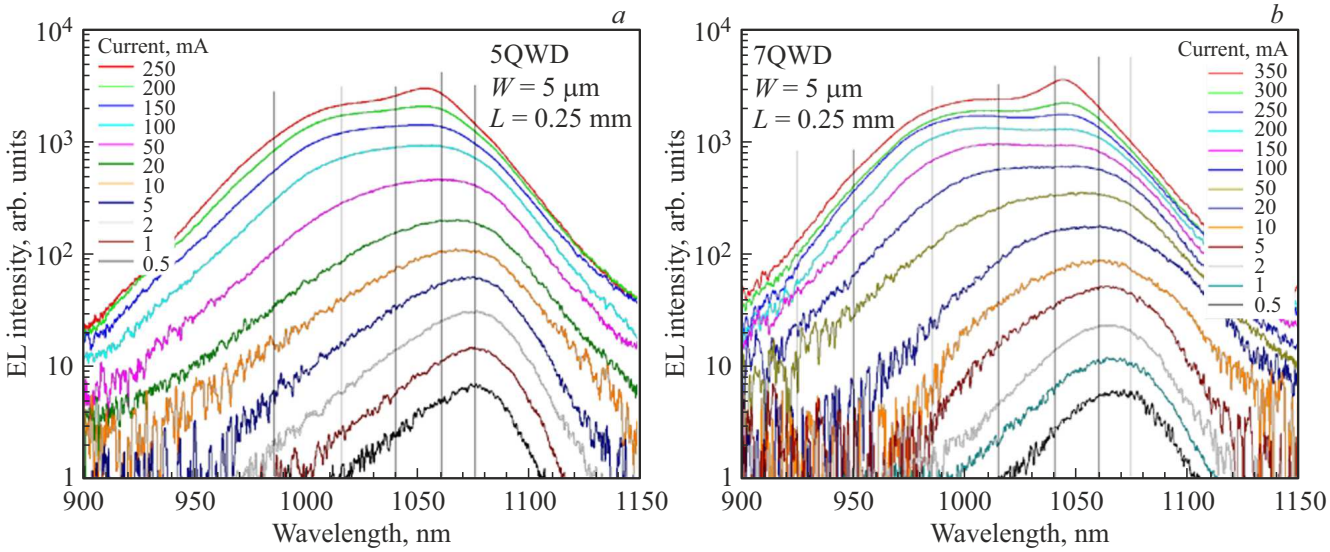

Figure 3. Electroluminescence spectra of 5QWD (*a*) and 7QWD (*b*) SLDs of 0.25 mm length at different pump currents. The vertical lines mark the nominal positions of the PL maxima of the QWD layers forming the active area. (A color version of the figure is provided in the online version of the paper).

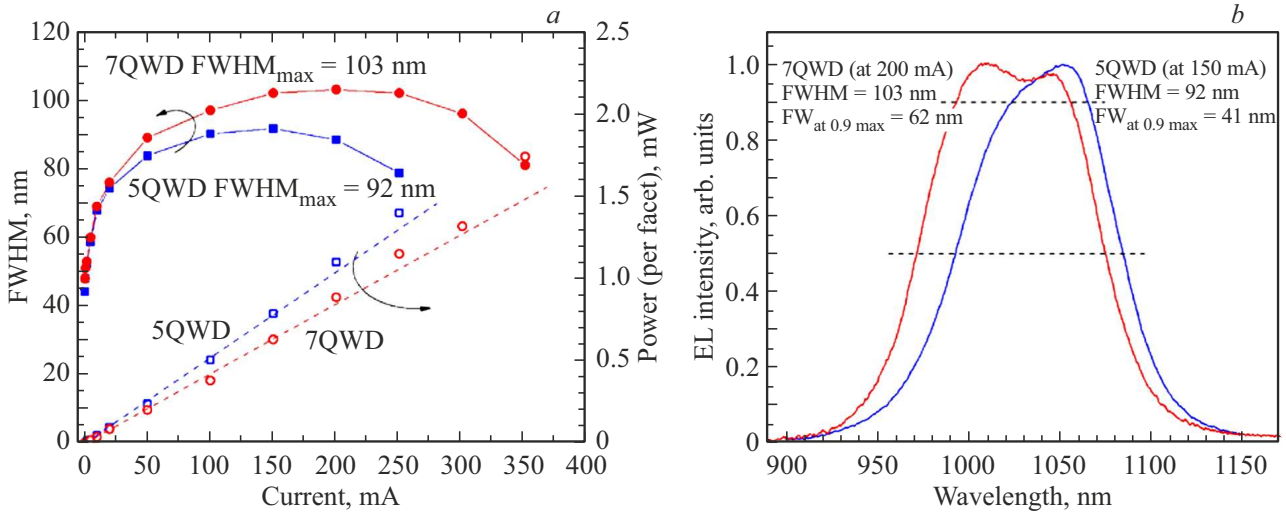

Figure 4. Dependences of the half-width of the electroluminescence spectra and emission power of 5QWD and 7QWD SLDs on the pump current (*a*). Normalized electroluminescence spectra of SLDs having maximum width (*b*).

In straight-stripe chips, which are actually edge-emitting lasers with Fabry–Perot resonator, laser generation at wavelength $\sim 1\,\mu$m occurs as the current rises. The spectral positions of the laser generation lines correspond to the energy range with maximum optical amplification in the multilayer active area, which, apparently, is achieved due to the superposition of the gain spectra of excited and ground states of several rows of QWDs. The lack of laser generation in the SLD means that using the tilted geometry of the SLD stripes allows the feedback to be suppressed quite effectively. The watt-ampere characteristic at the initial section has a linear dependence, changing with increasing current into a superlinear dependence characteristic of the stimulated emission mode. The output power at the maximum width of the EL spectra was 0.8 mW from one facet for both SLD 5QWD and SLD 7QWD.

In devices with a slightly longer resonator length, stimulated emission with a superlinear watt-ampere characteristic was observed starting from lower currents. Fig. 5 shows the EL spectra as well as the current dependence of the half-width spectra and emission power of 7QWD SLDs of length 0.3 mm. The stimulated emission occurs in the wavelength area corresponding to the QWD layers with PL peaks at 985, 1015, 1040, and 1060 nm. The maximum half-width of the EL spectra was 87 nm at a pump current of 250 mA and was smaller than the half-width of the 0.25 mm

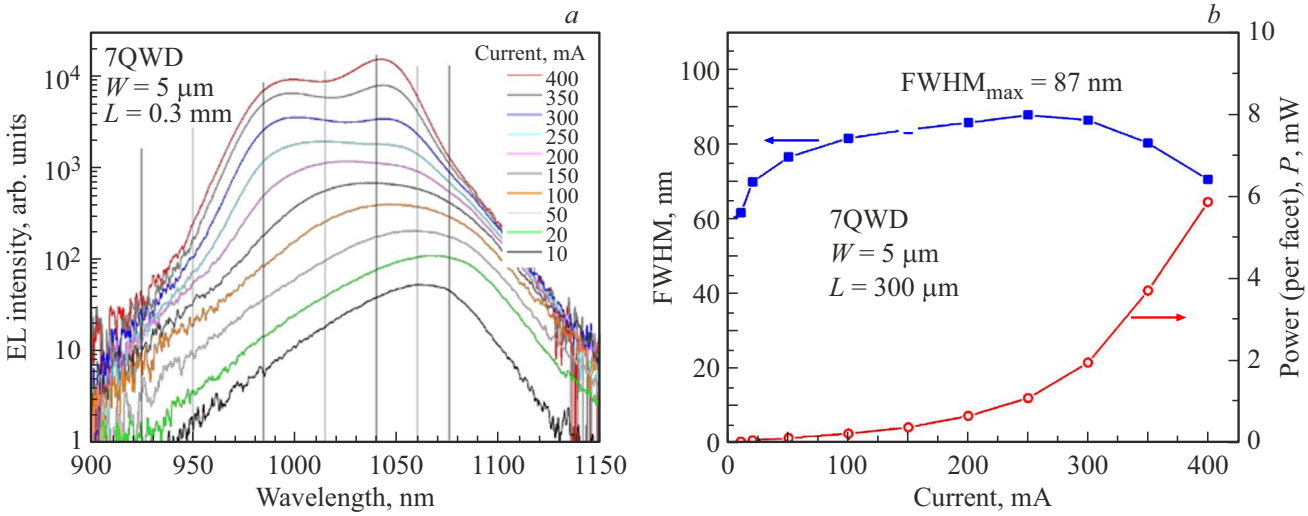

Figure 5. Electroluminescence spectra of 0.3 mm long 7QWD SLDs at different pump currents (*a*), current dependence of the half-width of electroluminescence spectra and emission power (*b*).

long SLD. The output power of radiation from one mirror at the maximum widths of the EL spectra was in the range 1.1–1.9 mW, which is larger than the corresponding output power of the SLD length 0.25 mm.

4. Conclusion

It is demonstrated that the use of multilayer arrays of QWDs with the radiation wavelength shifted relative to each other allows to obtain an EL spectrum with a width > 100 nm with a central wavelength $\sim 1\,\mu$m and a rather flat top. It is expected that the location of c QWD layers emitting in the short-wave part of the spectrum (925, 950 and 985 nm), closer to the *p*-cladding in order to increase their carrier occupancy will increase the relative contribution of these layers to the total emission spectrum and thereby increase its half-width. Higher output power can be achieved by increasing the length of the devices while effectively suppressing feedback, for example by applying anti-reflection coatings, using SLD designs with a laterally tapered waveguide, and adding an integrated optical amplifier section.

Funding

This study was supported by the Russian Science Foundation, project No. 23-72-00038, https://rscf.ru/project/23-72-00038/. O.I. Simchuk thanks the Ministry of Science and Higher Education RF (project 0791-2020-0002) for supporting the study of surface defects in samples by dark-field and light-field spectroscopy.

Conflict of interest

The authors declare that they have no conflict of interest.

References

[1] G.M. Hale, M.R. Querry. Appl. Opt., **12** (3), 555 (1973).
[2] Y. Yasuno, Y. Hong, S. Makita, M. Yamanari, M. Akiba, M. Miura, T. Yatagai. Opt. Express, **15** (10), 6121 (2007).
[3] A.F. Fercher, W. Drexler, C.K. Hitzenberger, T. Lasser. Rep. Progr. Phys., **66**, 239 (2003).
[4] M. Rossetti, P. Bardella, M. Gioannini, I. Montrosset. ECIO'08 Eindhoven — Proc. 14th Eur. Conf. on Integrated Optics and Technical Exhibition, Contributed and Invited Papers. Eur. Conf. on Integrated Photonics (2008).
[5] S.-H. Guol, Jr-H. Wang, Y.-H. Wu, W. Lin, Y.-J. Yang, C.-K. Sun, C.-L. Pan, J.-W. Shi. IEEE Photon. Technol. Lett., **21** (5), 328 (2009).
[6] A.E. Zhukov, V.M. Ustinov, A.R. Kovsh, A.Yu. Egorov, N.A. Maleev, N.N. Ledentsov, A.F. Tsatsul'nikov, M.V. Maximov, Yu.G. Musikhin, N.A. Bert, P.S. Kop'ev, D. Bimberg, Zh.I. Alferov. Semicond. Sci. Technol., **14**, 575 (1999).
[7] A. Kovsh, I. Krestnikov, D. Livshits, S. Mikhrin, A. Zhukov, J. Weimert. Optics Lett., **32** (7), 793 (2007).
[8] M.V. Maximov, A.F. Tsatsul'nikov, B.V. Volovik, D.S. Sizov, Y.M. Shernyakov, I.N. Kaiander, A.E. Zhukov, A.R. Kovsh, S.S. Mikhrin, V.M. Ustinov, Z.I. Alferov, R. Heitz, V.A. Shchukin, N.N. Ledentsov, D. Bimberg, Y.G. Musikhin, W. Neumann. Phys. Rev. B, **62** (24), 16671 (2000).
[9] S. Chen, W. Li, Z. Zhang, D. Childs, K. Zhou, J. Orchard, K. Kennedy, M. Hugues, E. Clarke, I. Ross, O. Wada, R. Hogg. Nanoscale Res. Lett., **10**, 340 (2015).
[10] S. Haffouz, M. Rodermans, P.J. Barrios, J. Lapointe, S. Raymond, Z. Lu, D. Poitras. Electron. Lett., **46** (16), 1144 (2010).
[11] Du Chang Heo, Jin Dong Song, Won Jun Choi, Jung Il Lee, Ji Chai Jung, Il Ki Han. Electron. Lett., **39** (11), 863 (2003).
[12] Z.Y. Zhang, R.A. Hogg, B. Xu, P. Jin, Z.G. Wang. Optics Lett., **33**, 1210–2 (2008).
[13] Aye S. M. Kyaw, Dae-Hyun Kim, Iain M. Butler, K. Nishi, K. Takemasa, M. Sugawara, David T.D. Childs, Richard A. Hogg. Appl. Phys. Lett., **122**, 031104 (2023).

[14] M.V. Maximov, A.M. Nadtochiy, S.A. Mintairov, N.A. Kalyuzhnyy, N.V. Kryzhanovskaya, E.I. Moiseev, N.Yu. Gordeev, Yu.M. Shernyakov, A.S. Payusov, F.I. Zubov, V.N. Nevedomskiy, S.S. Rouvimov, A.E. Zhukov. Appl. Sci., **10**, 1038 (2020).
[15] N.Yu. Gordeev, M.V. Maximov, A.S. Payusov, A.A. Serin, Yu.M. Shernyakov, S.A. Mintairov, N.A. Kalyuzhnyy, A.M. Nadtochiy, A.E. Zhukov. Semicond. Sci. Technol., **36**, 015008 (2020).
[16] S.A. Mintairov, N.A. Kalyuzhny, A.M. Nadtochy, M.V. Maksimov, V.N. Nevedomsky, L.A. Sokura, S.S. Ruvimov, M.Z. Shvarts, A.E. Zhukov. Semiconductors, **52** (10), 1131 (2018).
[17] Z.C. Wang, P. Jin, X.Q. Lv, X.K. Li, Z.G. Wang. Electron. Lett., **47** (21), 1191 (2011).
[18] X. Li, P. Jin, Q. An, Z. Wang, X. Lv, H. Wei, J. Wu, J. Wu, Z. Wang. IEEE Photon. Technol. Lett., **24** (14), 1188 (2012).
[19] A.F. Forrest, M. Krakowski, P. Bardella, M.A. Cataluna. Opt. Express, **27** (8), 10981 (2019).

Translated by Y.Deineka